Tissue Regeneration Enabled by 3D-Bioprinted Stromal Vascular Fraction

Alberto Augello [1], Giordano Perini [1,2], Margherita Montescagli [2], Giada Di Giulio[2], Valeria Ferrara[1], Antonio Minopoli[1,2], Davide Evangelista[2], Matteo Marras[2], Martina Palmieri, **Giulia Artemi[2]**, Anna Amelia Caretto[4], Stefano Gentileschi[4], Dania Nachira[5], Valerio Pontecorvi[6], Cristiano Spada[6], Loredana Gualtieri[6,7], Valentina Palmieri[3], Ivo Boskoski[6], Marco De Spirito [1,2,*] and Massimiliano Papi [1,2,*]

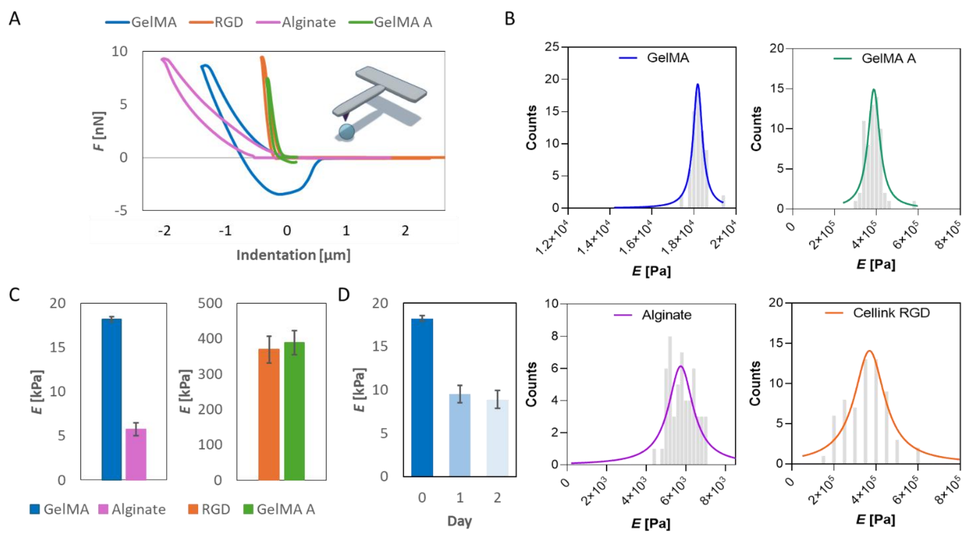
1 Fondazione Policlinico Universitario A. Gemelli IRCSS, 00168 Rome, Italy; 2 Dipartimento di Neuroscienze, Università Cattolica del Sacro Cuore, Largo Francesco Vito 1, 00168 Rome, Italy; 3 Istituto dei Sistemi Complessi, CNR, Via dei Taurini 19, 00185 Rome, Italy; 4 Plastic and Reconstructive Surgery, Fondazione Policlinico Universitario Agostino Gemelli IRCCS, Rome, Italy; 5 Thoracic Surgery, Fondazione Policlinico Universitario Agostino Gemelli IRCCS, Rome, Italy; 6 Digestive Endoscopy Unit, Fondazione Policlinico Universitario Agostino Gemelli IRCCS, Rome, Italy; 7 Department of Surgical Sciences, Sapienza University of Rome, Rome, Italy

At a glance

The stromal vascular fraction (SVF) is a heterogeneous, autologous cell population known for its regenerative, immunomodulatory, and proangiogenic properties. However, its therapeutic potential is often limited by the lack of structured delivery platforms capable of supporting its survival, organization, and coordinated action across multiple tissue compartments. This study aimed to develop and evaluate a 3D-bioprinted, patient-derived SVF construct designed to enhance epithelial, stromal, and vascular regeneration, addressing the broader clinical need for effective, multi-layer tissue repair in complex wounds and degenerative conditions.

Results

Four hydrogel matrices—alginate, Cellink-RGD, GelMA, and GelMA A—were mechanically and biologically screened using nanoindentation (Figure 1)



Representative force–indentation curves (Figure 1A) revealed distinct mechanical behaviors for each material, confirming their diverse viscoelastic responses under loading. Among the tested materials, Cellink-RGD and GelMA A displayed the highest stiffness, with Young's moduli of 350-400 kPa (Figure 1C), significantly exceeding those of alginate and GelMA. These values were extracted from the peak of the Lorentzian fit applied to the frequency distributions of individual nanoindentation measurements (Figure 1B). Interestingly, the moduli for Cellink-RGD and GelMA A were markedly higher reflecting the mechanical reinforcement contributed by nano-fibrillated cellulose and the ionic crosslinking of alginate. Despite their superior stiffness, these formulations may be less suitable for applications requiring a close mimicry of native soft tissue mechanics. From a biomedical perspective, the mechanical properties of GelMA are particularly relevant. Its stiffness falls within the lower range of native soft tissues such as the brain, liver, and tumor microenvironments, which typically exhibit moduli in the 1–30 kPa range. Importantly, we noticed an increasing compliance of GelMA over 48 hours of approximately 52% due to water absorption (Figure 1D).

BM-MSCs were selected as a representative model for early-stage hydrogel screening prior to employing SVF, due to their shared mesenchymal phenotype and comparable behavior in terms of adhesion, viability, and matrix interaction. Their relative homogeneity and widespread availability make them well-suited for evaluating the general cytocompatibility of biomaterials in a reproducible and controlled manner. BM-MSCs were bioprinted at a density of 2×10^6 cells/mL into four different hydrogels: alginate, Cellink-RGD, GelMA, and GelMA A (Figure 2).

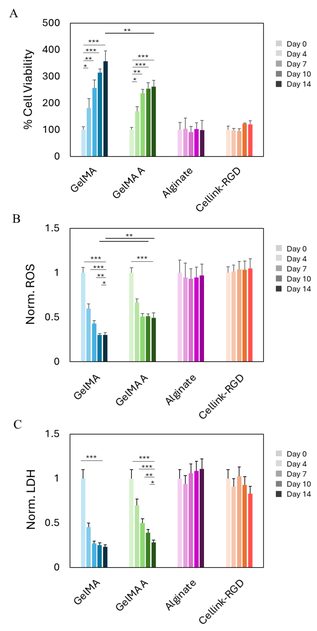


Figure 2 (right) A) Cell viability and B) Production of ROS over time. C) Cytotoxicity of the four different hydrogels on BM-MSCs over time measured by LDH release. Results are normalized by day 0 for each model.

A bioink was formulated by combining GelMA with freshly isolated SVF, and the resulting mixture was bioprinted and crosslinked. To evaluate the biological performance of the bioprinted constructs, we longitudinally assessed the state of the cellular component in terms of biocompatibility and cytotoxicity (Figure 3A-B). Another key element that should be taken into account for clinical translation is the long-term stability of bioprinted scaffolds. We therefore evaluated the rate of degradation of GelMA bioprinted with SVF at physiological pH (Figure 3C-D).

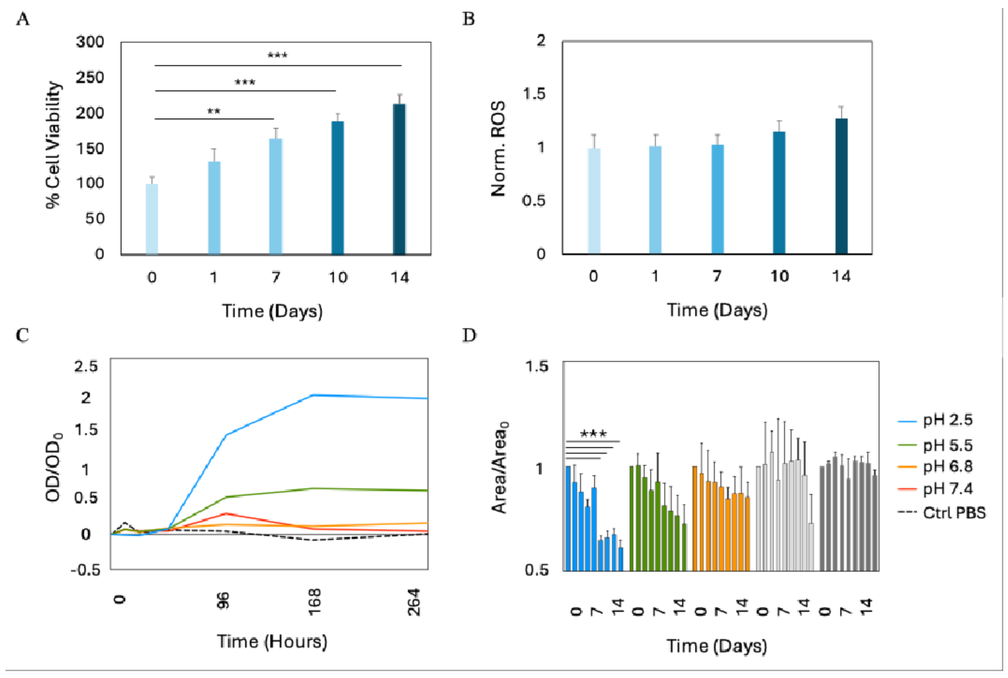


Figure 3 A) Viability of SVF bioprinted in GelMA over time. Results are expressed as % of day 0. B) Production of reactive oxygen species over time from SVF. Results are normalized to day 0. C) OD variation over 14 days. Results are reported with respect to the initial OD. D) Area variation over 14 days. Results are reported with respect to the initial area of each bioprinted model .

We monitored two key indicators of intestinal epithelial regeneration over time: (1) the viability and oxidative stress profile of the intestinal layer, and (2) the evolution of TEER, a measure of epithelial barrier integrity and tight junction function (Figure 4).

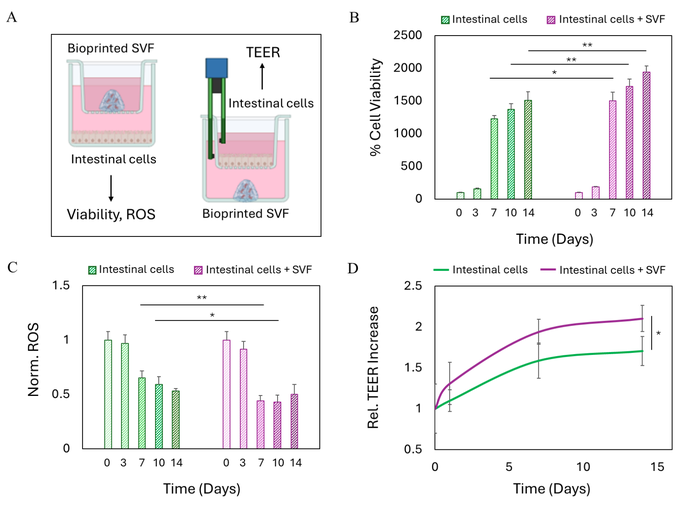


Figure 4 A) Schematic representation of the experimental setup. B) Cell viability of intestinal cells over time. C) Production of reactive oxygen species over time from intestinal cells with or without the presence of SVF. D) Increase in the electrical resistance of the intestinal barrier over time.

Evaluating fibroblast chemotaxis in response to bioprinted SVF offers important insights into the pro-regenerative capacity of the construct (Figure 5). We then conducted morphological evaluation of tubular structures following overnight to visualize cell viability and network architecture (Figure 6)

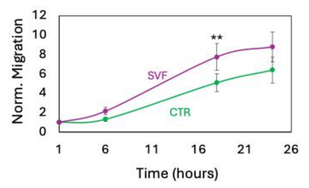
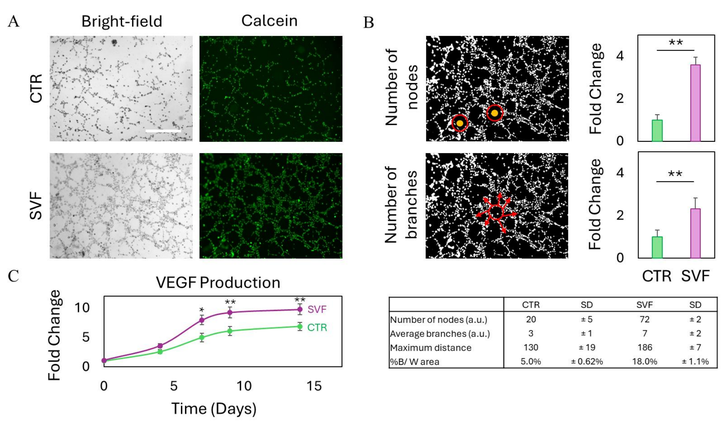


Figure 5 Quantitative analysis of migration of fibroblasts towards wound region over time.



	CTR	SD	SVF	SD
Number of nodes (a.u.)	20	± 5	72	± 2
Average branches (a.u.)	3	± 1	7	± 2
Maximum distance	130	± 19	186	± 7
%B/ W area	5.0%	± 0.62%	18.0%	± 1.1%

Figure 6 (right) A) Bright-field and fluorescence images of tube formation assay for endothelial cells in presence of SVF. Scalebar 300 µm. B) Quantitative analysis of tube formation in endothelial cells with and without SVF. C) Expression of VEGF over time with or without SVF.

Conclusions This study demonstrates that GelMA-based bioprinting of autologous SVF yields a multifunctional regenerative construct capable of promoting epithelial repair, stimulating stromal remodeling, and driving angiogenesis. These findings reinforce evidence on SVF's paracrine and immunomodulatory actions while extending its application to a structured 3D-bioprinted platform suitable for diverse tissue-engineering contexts.

TERMIS EU-Chapter 2026 PALMA DE MALLORCA 21-24 APRIL / SPAIN

The research leading to these results has received funding from MULTIPROBE - Real-time endoscopic diagnosis and therapy of gastrointestinal tumors through multimode nonlinear fibers CUP: J83C26000040006 PI Prof. Massimiliano Papi massimiliano.papi@unicatt.it

Gemelli Fondazione Policlinico Universitario Agostino Gemelli IRCCS Università Cattolica del Sacro Cuore

erc European Research Council Established by the European Commission



Perini, Giordano, et al. "3D-Bioprinting of Stromal Vascular Fraction for Gastrointestinal Regeneration." *Gels* 11.9 (2025): 712.

termis EUROPE